

Influence of bottom ash and red mud additions on self-leveling underlayment properties

H. D. S. Carvalho^{1*}, J. C. Rocha¹, M. Cheriaf¹

¹Federal University of Santa Catarina, Department of Civil Engineering, Waste Recovery Laboratory, Campus Trindade, 88040-900, Florianópolis, SC, Brazil

Abstract

Self-levelling underlayments (SLUs) based on Portland cement (PC) are susceptible to cracking due to drying shrinkage. The present study evaluated the influence of binder contents on systems consisting of calcium aluminate cement (CAC), PC, and a source of calcium sulfate (C\$), derived from the flue gas desulfurization process (FGD), on the mechanical (flexural and compressive) properties and drying shrinkage of SLUs. The main objective was to analyze the influence of replacing limestone filler (LF) by bottom ash (BA) and red mud (RM) wastes on the properties of SLUs based on the CAC/FGD/PC (56/24/20) binder system. For this purpose, mini-slump flow, setting times, water absorption, mechanical (flexural and compressive) strength, linear shrinkage, and X-ray diffraction essays were performed. The replacement at a level of 0.2 filler with wastes reduced linear shrinkage while replacing 0.3 filler level provided greater initial (1 day) compressive strength.

Keywords: self-levelling underlayments, mechanical strength, bottom ash, red mud, drying shrinkage.

INTRODUCTION

Self-levelling underlayments (SLUs) are materials that have high fluidity, with self-leveling capacity, only under their own weight, without the need for compaction [1-3]. The high fluidity provides a good surface finish [1, 2, 4] and reduces defects such as cracks and internal voids. In addition to self-leveling, this system has advantages over the conventional system, such as faster curing, greater initial mechanical strength, faster service execution [1], pumpability [2], and thin application [5, 6]. Given these characteristics, the self-leveling system began to arouse interest in the production of screeds or floors, with various applications in civil construction, such as in new and old, residential and commercial buildings, parking lots, schools, factories, hospitals, among others [1, 3, 5]. The application of SLUs, in a thin layer, over an area of several square meters, implies a large surface area exposed to the environment and in contact with the substrate. The loss of water by evaporation, due to the exchange of humidity with the environment, the absorption of water generated by the substrate, and the consumption of water generated by the hydration reactions, can cause a very fast drying of the material [5]. Fast drying can trigger problems related to drying shrinkage, such as cracking and/or curling at the corners (curling). These phenomena are mainly due to the internal moisture gradient of the mortar due to drying shrinkage [6, 7].

Drying shrinkage occurs due to loss of water mass by evaporation. According to the diffusion phenomenon, the

exchange of humidity in the material, initially saturated, occurs until the moment of equilibrium with the relative humidity of the environment. As the saturation degree of the material reduces, menisci form in the capillary pores, which cause an unbalance of internal stress [8]. The state of stress unbalance in the pores is promoted mainly by the phenomena of surface tension, energies at the interfaces, and disjoining pressure, which lead to material contraction in the case of shrinkage [8]. Therefore, the drying shrinkage of self-leveling underlayments based on Portland cement (PC) tends to be higher than the conventional mortar screed system [9]. To satisfy the performance demands of SLUs [10], the use of cements with aluminates, such as calcium sulfoaluminate cement (CSA) and calcium aluminate cement (CAC), has shown good performance in tests that evaluated the mechanical (flexural and compressive) strength and the dimensional variation, mainly when used in conjunction with other binders [1-4]. The binder system composed of CSA and low content of PC provides less drying shrinkage, compared to the system consisting only of PC [6], since the main hydration product is ettringite, which has an expansive property in the presence of portlandite (CH) [11]. For the binder system composed of CSA and a source of calcium sulfate (C\$), the SLUs showed higher initial compressive strengths (1 day=1d) and lower drying shrinkage at advanced ages (28d), when compared to dosed SLUs only with CSA, mainly in mixtures with a CSA/C\$ (anhydrite) ratio of 2.33 [12]. For the SLUs composed by the ternary system CSA/C\$/PC, the X-ray diffraction analyses indicate that the content of ettringite formed increases with the increase of the C\$ content, up to the ternary ratio CSA/C\$/PC of 10/12/8, in mass [1].

Similar performance to the binder system composed of CSA and PC was observed in a ternary composition of

*hdsc2012@gmail.com

<https://orcid.org/0000-0002-4690-3374>

binders formulated with CAC, a source of C\$ and PC [3, 4]. The main product of the hydration reaction is ettringite. The ternary system of binders CAC/C\$/PC has demonstrated efficiency in compensating the drying shrinkage and increasing the initial strength of SLUs, provided that the types and contents of the binders are dosed properly [2, 3]. For example, CAC/C\$/PC system with high C\$ contents of the hemihydrate type can generate high expansion rates, which result in cracking or even destruction of the material [3]. On the other hand, the SLUs produced with the ternary system CAC/C\$/PC with a predominance of PC presented a better performance than the SLUs composed of the binary system CAC/PC with high contents of PC. In this case, increasing the C\$ content from 0 to 6% provides a reduction in the value of shrinkage, especially in SLUs made with anhydrite and hemihydrate [2]. For the CAC/C\$/PC system with small and medium levels of PC, the SLUs formulated with the C\$ of the hemihydrate type showed greater dimensional variation than the C\$ of the anhydrite and dihydrate types and may present cracking, especially in the formulations with mean PC contents [3]. Furthermore, the CAC/C\$/PC system dosed with the anhydrite has shown better performance on the fluidity of SLUs in relation to the hemihydrate and dihydrate [2], for small, medium [3], and high [2] PC contents, due to the slow rate of dissolution of anhydrite [2, 13]. Compositions with low PC contents presented shorter start and end times of setting, indicating a more efficient hardening and curing process than systems with medium [3] and high PC contents [2].

The world scenario has shown interest in the recovery of by-products or industrial waste that can replace raw materials, benefit the properties of SLUs, reduce environmental impacts, and add value to the material. FGD (*flue gas desulfurization*) gypsum is a residue generated during the desulfurization process of SO₂ gas in coal-based thermoelectric plants [14, 15]. This residue aroused potential for SLU production, as it has a chemical composition similar to natural gypsum [16]. Bottom ash (BA) is a residue generated by the coal combustion process in thermoelectric plants. The coal is burned and pulverized in boilers, where the coarser and heavier particles are deposited at the bottom, being later sent to the deposition basins [17, 18]. Bottom ash can reduce drying shrinkage in concrete [18] and mortar [19] based on PC, through the effect of internal curing. This effect occurs because the bottom ash particles present high

initial water absorption due to their high porosity [19-21]. The phenomenon of internal curing consists of the gradual release of the water initially absorbed, during the drying process, allowing the material's humidity to remain at a higher level or to reduce more slowly [9, 22]. Red mud (RM) is a residue from the aluminum production industry, derived from the bauxite refining process to produce alumina, through Bayer method. Normally, the red mud is destined for waste ponds, which implies the occupation of considerable natural areas and an increase in the risk of triggering serious environmental impacts [23-26]. Red mud showed potential to reduce drying shrinkage in concrete [23] and autogenous shrinkage in mortars [24] due to internal curing effect, promoted by the porosity and high surface area of its particles.

The main objective of this study was to analyze the influence of replacing the limestone filler (LF) by the bottom ash and red mud fines on the properties of SLUs based on the CAC/FGD/PC ternary system. For that, tests of fluidity, setting times, water absorption, mechanical (flexural and compressive) strength, and linear drying shrinkage were conducted on the CAC/FGD/PC/LF, CAC/FGD/PC/BA, and CAC/FGD/PC/RM systems. Besides, X-ray diffraction analyses were performed on the pastes of these systems at 28 days of curing to evaluate the main crystalline phases formed due to the replacement of LF by BA and RM.

MATERIALS AND METHODS

The ternary system of binders used in this study was composed of aluminous cement (CAC) of the Fondu Lafarge type, Portland cement (PC), PC V type - high early strength (HES), and FGD gypsum (FGD). The FGD and bottom ash (BA) were donated in their raw state by coal-based thermoelectric plants installed in the South Region of Brazil. The FGD was calcined at 650 °C for 4 h to eliminate possible impurities and, mainly, obtain a calcium sulfate source similar to anhydrite II (natural), based on the methodology adopted to synthesize phosphoanhydride, from phosphogypsum [13]. The red mud (RM), a residue from aluminum production, was calcined at 600 °C for 1 h to increase its pozzolanic activity [26]. The calcination step of the residues (FGD and RM) was conducted in a muffle furnace (KK 170 SO 1059), adopting a heating rate of 10 °C/min until reaching the maximum

Table I - Physical properties of binders and additions.

Property	CAC	PC	FGD	LF	BA	RM
D ₅₀ (µm)	2.198	0.998	2.636	2.488	2.064	0.781
Blaine surface area (m ² /g)	0.39	0.42	=	=	=	=
BET surface area (m ² /g)	-	-	5.00	1.76	3.79	30.22
Absolute gravity (g/cm ³)	3.02	3.25	2.87	2.93	2.94	3.02
Apparent gravity (g/cm ³)	2.94	3.13	2.80	2.87	2.22	2.84
Porosity (%)	3.69	2.65	2.44	2.05	23.47	5.96

Table II - Chemical compositions (wt%) of binders and additions.

Oxide	CAC	PC	FGD	LF	BA	RM
CaO	27.39	55.24	29.78	52.55	1.50	1.09
SiO ₂	3.76	21.42	6.19	6.54	56.01	23.40
Al ₂ O ₃	66.71	4.57	0.72	-	24.65	17.35
SO ₃	0.004	4.34	51.00	0.09	1.07	0.21
MgO	0.64	8.19	3.16	-	-	-
Fe ₂ O ₃	0.20	2.35	0.25	1.07	5.14	41.63
K ₂ O	0.21	0.97	0.28	0.52	2.87	0.09
TiO ₂	0.03	0.26	-	0.18	1.13	5.31
ZrO ₂	0.30	-	-	-	0.07	1.09
CO ₂	0.41	2.37	8.56	38.84	7.33	9.31

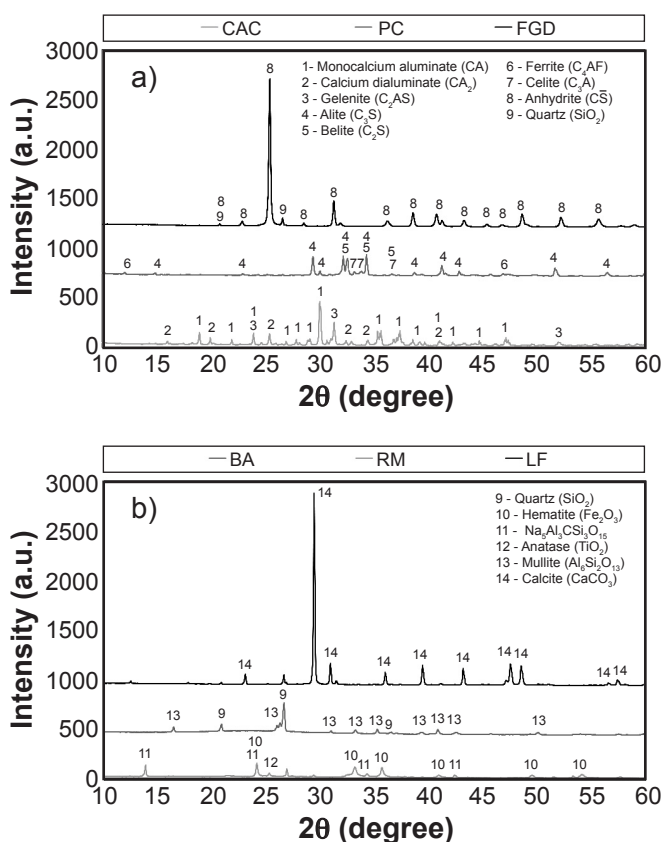


Figure 1: XRD patterns of the binders (a) and additions (b).

temperature. After reaching the final calcination time, the muffle was turned off, and the residues were kept inside until the internal temperature stabilized with environment temperature. The BA was dried, at 105 °C for 48 h, ground, and sieved. The reduction in the size of the bottom ash particles increases the pozzolanic activity and reduces the porosity [17]. Consequently, the initial water absorption rate can be significantly reduced [19], which benefits the fluidity. Bottom ash grinding was performed in 5 cycles of 100 min by a ball mill (MU 75, Siti), operating with 425 steel balls

at a speed of 40 rpm. Finally, the bottom ash was sieved to guarantee particles with dimensions finer than 0.075 mm mesh sieve. After the treatments, BA and RM fines were used to replace the calcitic limestone filler, dried at 105 °C. The superplasticizer (SP) additive with a polycarboxylate chemical base was used to obtain high fluidity. In contrast, the viscosity modifier (VMA) additive, based on tartaric acid, was used to guarantee the high cohesion of the mixtures and avoid signs of exudation and/or segregation. In turn, the setting retardant additive (SR), based on a biopolymer, was used to adjust the workability time of the mortar. The natural sand used presented characteristic dimensions of a maximum of 1 mm and a minimum of 0.15 mm.

The physical properties of the binders and additions are shown in Table I. The surface areas of the cements (CAC and PC) were determined by the Blaine method, while the surface areas of the residues (FGD, BA, and RM) and of the filler (LF) were determined by a surface area analyzer (Autosorb-1, Quantachrome). The water pycnometer method determined the apparent specific gravity, while the absolute specific gravities were determined by a helium gas pycnometer (AccuPyc II 1340, Micromeritics). Porosity was calculated from the ratio between the apparent and absolute specific gravities. The granulometric compositions were determined using a particle size distribution (PSD) analyzer (Lumisizer, Lum). The RM particles presented high surface area due to the small dimensions of their particles. The BA particles showed mean particle size similar to those of CAC, correspondingly larger in relation to PC, and slightly smaller in relation to LF and FGD. The BA particles showed high porosity, thus contributing to the fact that the replacement of LF by BA, in mass, implied a greater volume of addition per cubic meter of SLU produced. Therefore, the replacements of LF by BA and RM were performed in volumetric proportions. The chemical analyses of the binders and additions were determined using an energy dispersive X-ray fluorescence spectrometer (EDX 7000, Shimadzu). The results of these analyses are shown in Table II. The values of loss on ignition (CO₂) were determined by calcination at 900 °C for 4 h through the same muffle and the same heating and cooling rates adopted to calcine the residues (FGD and RM). The mineralogical characterization of the binders and additions was performed using an X-ray diffractometer (X'Pert Pro, Panalytical; CuK α radiation of 1.54 Å). The diffractograms were determined using an angular step of 0.02° and a 2θ analysis range ranging from 10° to 60°. The diffraction patterns of the binders and additions are respectively shown in Figs. 1a and 1b. Mineralogical analyses indicated that RM was composed of hematite (Fe₂O₃), Na₅Al₃CSiO₁₅, quartz (SiO₂), and anatase (TiO₂), while BA was composed of quartz and mullite (Al₆Si₂O₁₃). On the other hand, LF was made up mainly of calcite. CAC was composed of monocalcium aluminate (CA), calcium dialuminate (CA₂), and gehlenite (C₂AS) phases. The PC was constituted by the phases alite (C₃S), belite (C₂S), ferrite (C₄AF), and celite (C₃A), where C=CaO, S=SiO₂, A=Al₂O₃, and F=Fe₂O₃. The FGD gypsum showed XRD patterns similar to natural anhydrite.

Table III - Mixtures compositions (kg/m³).

Binder		SLU (kg/m ³)						w/f	Cement consumption CAC+PC (kg/m ³)
CAC/FGD	PC (%)	CAC	FGD	PC	LF	Sand	Water		
2.33	10	384.36	164.73	61.01	122.02	1098.18	335.56	0.46	445.37
		375.90	161.10	59.67	179.00	1074.00	328.17	0.42	435.57
	20	343.42	147.18	122.65	122.65	1103.84	337.28	0.46	466.07
		334.71	143.45	119.54	179.31	1075.84	328.73	0.42	454.24
3.00	10	412.01	137.34	61.04	122.08	1098.70	335.71	0.46	473.05
		402.94	134.31	59.69	179.08	1074.50	328.32	0.42	462.63
	20	368.10	122.70	122.70	122.70	1104.31	337.43	0.46	490.80
		358.76	119.59	119.59	179.38	1076.28	328.86	0.42	478.35
4.00	10	439.69	109.92	61.07	122.14	1099.23	335.87	0.46	500.76
		430.00	107.50	59.72	179.17	1075.00	328.47	0.42	489.72
	20	392.81	98.20	122.75	122.75	1104.78	337.57	0.46	515.56
		382.84	95.71	119.64	179.46	1076.73	329.00	0.42	502.47

For all compositions: binders:sand ratio=1:1.80; w/c (water/binders) ratio=0.55.

The fluidity of the SLUs was evaluated through mini-slump flow test on a glass plate, as recommended by ASTM C1708 standard [10]. The contents of SP and VMA additives were dosed to obtain a minimum flow of 110 mm and a maximum of 120 mm to guarantee the high cohesion of the mixture without compromising the self-leveling of the mortars. The start and end times of setting of the SLUs were determined using the Vicat needle method, in accordance with ABNT NBR 16607 standard [27]. According to note 11 of ASTM C1708 [10], the setting time of fast drying self-leveling underlayments normally varies between 1 and 3 h. Thus, the SR additive content was dosed to adjust the start time of setting between 90 and 180 min and the maximum end of setting time of 240 min, in order to provide a good amount of time for the application of the material, without compromising the desired rapid cure. The contents of the additives were measured in relation to the total mass of the CAC/FGD/PC system. The apparatus used to conduct the mixing procedure was standardized in accordance with ABNT NBR 7215 standard [28]. However, the molding was conducted without any consolidation due to the self-leveling capacity of the mortars produced. The flexural strengths were determined on three prismatic samples (40x40x160 mm). In comparison, the compressive strengths were determined on the six samples from the flexural strength test, according to the methodology defined in ABNT NBR 13279 standard [29]. Linear drying shrinkage was measured on three prismatic samples (25x25x285 mm), in accordance with ASTM C490 guidelines [10]. The curing of the mortar samples was conducted in the air, in a controlled temperature environment of 23±2 °C and relative humidity above 70%. In the case of the mortar samples destined to the shrinkage test, the curing was conducted in an environment with a controlled temperature of 23±2 °C and a controlled relative humidity of 55±5%. The composition of the reference CAC/FGD/

PC ternary binder system was determined considering the flows, setting times, mechanical (flexural and compressive) strength, and linear drying shrinkage suitable for SLUs. Therefore, the mortars constituted by the CAC/FGD/PC/LF systems were produced from three CAC/FGD ratios (2.33, 3.00, and 4.00), two PC contents (10% and 20%), and two levels of LF addition (0.2 and 0.3), in relation to the mass of the CAC/FGD/PC system. The w/c (water/binders) ratio and the aggregate proportion (binders/sand) were kept constant, while the w/f [water/(CAC+FGD+PC+LF)] ratio varied as a function of the addition content (Table III).

To evaluate the influence of residues on the properties of SLUs, mortars with 100% volumetric substitution of LF by BA and RM were produced. In these SLUs, water absorption tests were also performed by immersion, in cylindrical samples (D=50 mm and h=100 mm), according to the methodology established in ABNT NBR 9778 standard [30]. The composition and w/c ratio were the same adopted in the reference SLUs (CAC/FGD/PC/LF). Also, mineralogical analyses were performed on the pastes of the CAC/FGD/PC/LF, CAC/FGD/PC/BA, and CAC/FGD/PC/RM systems, at 28 days of curing, through an X-ray diffractometer (XRD, MiniFlex II, Rigaku), which contained a tube with a copper anode (1.54 Å CuK α radiation). The diffractogram records were performed using an angular step of 0.02° and 2 θ ranging from 6° to 12° since the main peak of ettringite, where the relative intensity is 100% (ICSD file 16045), occurs near the angle 2 θ of 9°. Qualitative analysis was performed using a software (X'Pert HighScore Plus, PANalytical) based on the standard diffractograms available in the database (PDF2 2013). In turn, the semi-quantitative analysis of the crystalline phases was performed according to the integrated intensity method [31], with the aid of a software (Origin Pro, OriginLab). Sample preparation for XRD tests was performed after 28 days of curing when the

pastes were fragmented, and the central parts of the samples were immersed in isopropyl alcohol for 72 h at 23 ± 2 °C to interrupt the hydration of the binders. After immersion in isopropanol, the samples were air-dried for 2 h to evaporate the excess alcohol and then oven-dried at 40 °C for 72 h, based on the methodology adopted by Rocha [32]. After drying in an oven, the paste fragments were ground using a mortar and pestle and sieved to obtain dimensions below 75 μm . Finally, the samples were stored in a desiccator until the test date. The freezing methodology with isopropanol was adopted because it is one of the least aggressive techniques to the material microstructure [33].

RESULTS AND DISCUSSION

Self-leveling underlayments with limestone filler addition

Flows and setting times: the results of the flow tests (e) and the start (SS) and end (ES) times of setting of the reference mortars (LF) are presented in Table IV. The start times of setting were in accordance with the values mentioned in note 11 (1 and 3 h) of ASTM C1708 [10]. The different compositions of binders tested did not demonstrate a relevant influence on the start times of setting, with a maximum variation of 20 min, due to the action of the SR additive. However, mortars with 20% PC had shorter end times of setting, indicating a faster hardening process than mortars with 10% PC. This result pointed to a similar trend to the CAC/PC binary system, where the increase from 10% to 20% PC reduced the setting times in mortars. It is worth mentioning that the variation in setting times depends on the type of PC used, mainly with regard to the content and type of C\$. The phenomena responsible for the short setting time

of the CAC/PC system are still not completely understood. Nevertheless, factors such as the acceleration of hydration reactions of ettringite and/or aluminate phases (CA, CA₂, and C₃A) may be related [34].

Mechanical (flexural and compressive) strengths: the results of flexural tensile strength and compressive strength of the reference SLUs (LF) at 1, 7, and 28 days of curing are respectively presented in Figs. 2a and 2b. According to the values of compressive strength, at 1 (22 ± 7 MPa), 7 (32 ± 7 MPa), and 28 (39 ± 9 MPa) days of curing, and flexural strength at 1 (4.5 ± 1.2 MPa) and 7 (7.5 ± 2.5 MPa) curing days, established in ASTM C1708 [10], mortars with 10% PC showed unsatisfactory compressive strength results at initial age (1d), while mortars with 20% PC and CAC/FGD ratio of 4.00 presented unsatisfactory flexural strength results at 7 days. Among the mixtures tested, only SLUs with 20% PC and CAC/FGD ratios of 2.33 and 3.00 showed satisfactory results in terms of compressive and flexural strengths at 1, 7, and 28 days of curing. At the initial age (1d), SLUs with 20% PC showed higher compressive and flexural strengths, in all CAC/FGD ratios and tested addition contents. Therefore, increasing the PC content from 10% to 20% of the CAC/FGD/PC system promoted a better initial curing process (1d). This result was consistent with the lowest end times of setting observed in SLUs with 20% PC and may be related to the type of PC used in this study.

For the CAC/C\$/PC system with the predominance of CAC and availability of C\$, the main hydration reactions occur according to Eqs. A to C [4]. In addition, the hydration reactions of the PC phases occur depending on their type and content. Portland cement of high early strength (PCV-HES) used in this study is mainly constituted by the alite phase (C₃S), being the main responsible for the development of

Table IV - Flow and settings times of SLUs with LF addition.

CAC/FGD	PC (%)	LF	SP (%)	VMA (%)	SR (%)	F (cm)	SS (min)	ES (min)
2.33	10	0.2	0.27	0.07	0.05	11.7	110	190
		0.3	0.30	0.04	0.05	11.6	95	170
	20	0.2	0.29	0.07	0.05	11.8	90	130
		0.3	0.32	0.04	0.05	11.8	95	130
3.00	10	0.2	0.26	0.07	0.05	11.7	100	170
		0.3	0.29	0.07	0.05	11.8	95	170
	20	0.2	0.28	0.07	0.05	11.5	100	135
		0.3	0.31	0.07	0.05	11.7	90	125
4.00	10	0.2	0.25	0.10	0.05	11.6	105	180
		0.3	0.28	0.07	0.05	11.9	100	170
	20	0.2	0.27	0.07	0.05	11.5	105	145
		0.3	0.30	0.07	0.05	11.7	100	130

CAC: calcium aluminate cement; FGD: gypsum derived from flue gas desulfurization process; PC: Portland cement; LF: limestone filler; SP: superplasticizer additive; VMA: viscosity modifier additive; SR: setting retardant additive; F: flow; SS: start time of setting; ES: end time of setting.

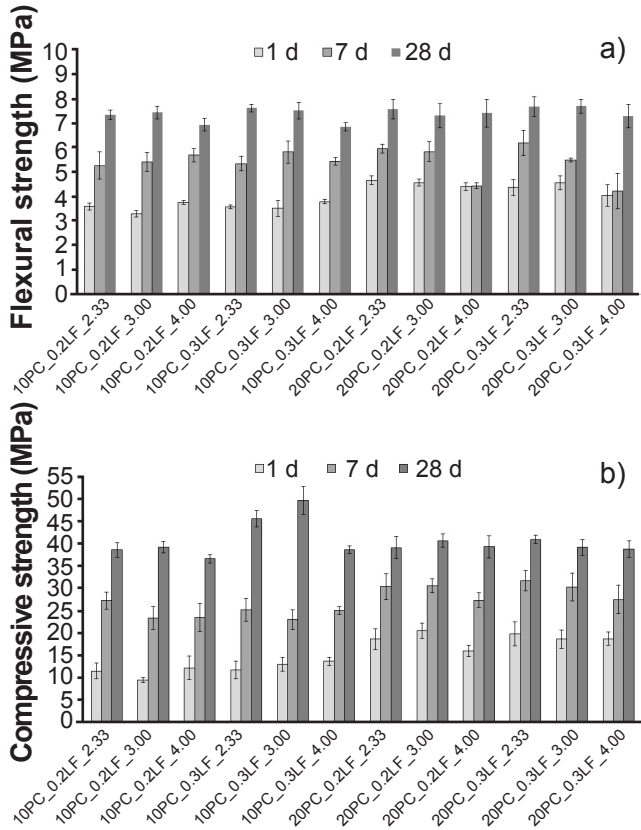
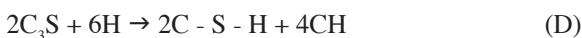
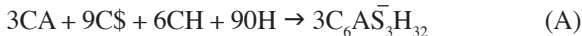


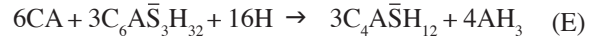
Figure 2: Flexural (a) and compressive (b) strengths of SLUs with LF addition.

the initial mechanical strengths in PC-based systems [35]. Even in alumina-rich systems (CSA/C\$/PC), the initial reactivity of alite is high [36]. Therefore, SLUs with 20% PC may have formed a higher C-S-H content (Eq. D), which may have contributed to the increase in initial mechanical strengths. Furthermore, the increase in PC content may have accelerated the formation of ettringite (Eq. A) due to the greater availability of portlandite (CH). It is worth mentioning that Eq. A results in a higher content of formed ettringite but demands a higher consumption of C\$, in relation to Eqs. B and C.



Considering the standard deviations for a constant PC content, the SLUs with CAC/FGD ratios of 2.33 and 3.00 presented similar mechanical strength values at all ages tested. At 7 days of curing, the SLU with the lowest level of FGD (16%), constituted with 20% PC and CAC/FGD ratio of 4.00, presented the lowest flexural strength value at 7 days of curing. At 28 days of curing, SLU with 18% FGD, composed with 10% PC and CAC/FGD ratio of 4.00,

showed lower mean values of mechanical strength at 28 days of curing compared to CAC/FGD ratios of 2.33 and 3.00. One hypothesis for this occurrence is that the increased availability of C\$ may have accelerated the curing process (Eq. A). Furthermore, these results may also be related to the phase conversions of the hydration products. After consumption of the C\$ source, the conversion of ettringite to monosulfate can occur, according to:



The ettringite phase has a larger volume than the monosulfate phase due to the loss of sulfate and water molecules [37]. Thus, when the conversion of ettringite into monosulfate occurs, the porosity increases and, consequently, the mechanical strength tend to decrease [37, 38]. Therefore, the lower values of mechanical strength obtained in SLUs with lower FGD contents (CAC/FGD of 4.00) may also be related to the conversion of ettringite into monosulfate. In this study, the increase in the addition content implies a lower content of binders and aggregate per volume of mortar, but also implies a lower water content (w/f). Therefore, the reduction in the w/f ratio was one of the reasons why the mechanical strengths did not decrease in SLUs with lower levels of binders (0.3 LF). Also, the packing and nucleation effects promoted by LF particles can reduce the porosity of mortars [39]. The increase in the addition content promoted an increase in the compressive strength values of SLUs with 10% PC, at 28 days of curing, mainly for the CAC/FGD ratios of 2.33 and 3.00. In this case (10PC_0.2LF), the chemical effect of the LF particles may also have contributed to an increase in the mechanical strength in systems with high CAC contents (>63%) since the presence of calcite can promote a better stabilization of ettringite. As the availability of C\$ is reduced, the aluminate phases (CA, CA₂, and C₃A) react with the calcite phase (CaCO₃) to form hemicarboaluminate (Eq. G), preventing or reducing the rate of conversion of ettringite to monosulfate (Eqs. E and F) [40]:



Linear drying shrinkage: the results of linear drying shrinkage of the reference SLUs (LF) with 10% and 20% PC are respectively shown in Figs. 3a and 3b. According to ASTM C1708 [10], the mean values of linear drying shrinkage of SLUs at 3, 7, 14, and 28 days of curing are, respectively, -0.089%, -0.116%, -0.126%, and -0.129%. The mean values of linear shrinkage obtained in this study at 28 days of curing were 10 times lower than the values of linear shrinkage recommended for 3 days of curing by ASTM C1708 [10]. Therefore, all SLUs produced showed low shrinkage rates by drying. For 10% PC, SLUs with 0.3 LF addition showed slightly lower linear shrinkage values after 14 days, compared to SLUs with 0.2 LF addition, and the CAC/FGD ratio showed no influence on the linear

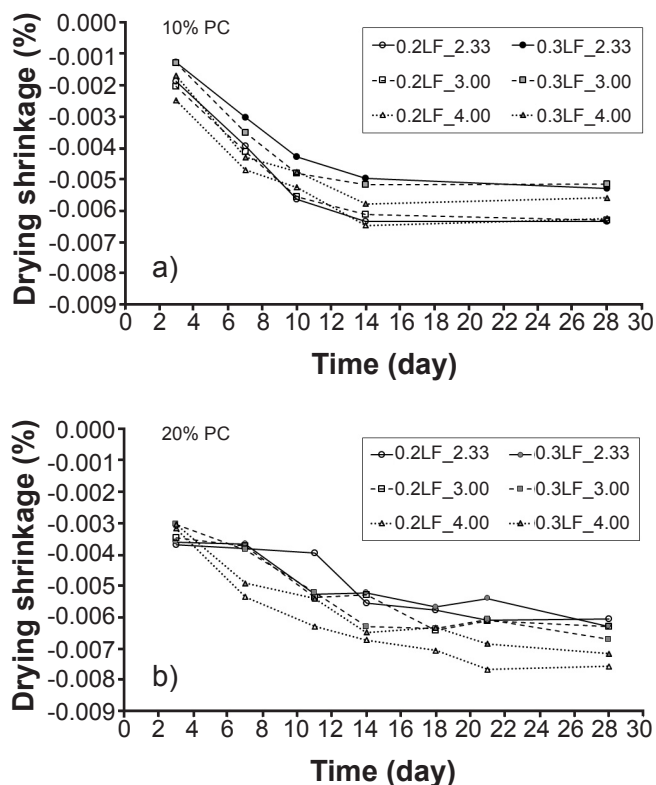


Figure 3: Drying shrinkage of SLUs with addition of LF and 10% PC (a) or 20% PC (b).

shrinkage of mortars. SLUs with 20% PC showed higher values of initial linear shrinkage (2d) compared to SLUs with 10% PC. This result may be related to the increase in the C-S-H content and/or the reduction in the ettringite content as a function of the increase in the PC content in the system. For 20% PC, SLUs with a CAC/FGD ratio of 4.00 showed greater linear shrinkage. On the other hand, mortars with 20% PC and CAC/FGD ratio of 2.33 showed better dimensional stability after 14 days of curing. Furthermore, mortars with a CAC/FGD ratio of 2.33 allow for incorporating a higher FGD content, which is a favorable parameter for sustainability and for reducing the value added to the material. Considering that all SLUs produced showed small values of linear shrinkage and that SLUs with 20% PC showed higher values of initial mechanical (flexural and compressive) strength, the production of SLUs with BA and RM was conducted in CAC/FGD/PC ternary system with 20% PC and CAC/FGD ratio of 2.33.

Self-leveling underlayments with additions of LF, BA and RM

Flows and setting times: the results of the flow and setting times of the SLUs with the addition of LF, BA, and RM are presented in Table V. According to ASTM C1708 [10], the flows of self-leveling underlayments must vary between 12.5 and 15 cm. However, the mortars with higher bottom ash contents showed signs of exudation for flows greater than 12.5 cm. The exudation of this system (0.3_BA) was caused by the gradual release of water initially absorbed by

the BA particles due to their high porosity. For this reason, the flow values were defined between 11 and 12 cm, aiming to guarantee high fluidity and cohesion, which provided the mortar with self-leveling without signs of exudation and/or segregation. The replacement of LF by RM increased the demand for SP additive due to the high surface area of the red mud particles, while the replacement of LF for BA increased the demand for VMA additive to avoid exudation. The replacement of LF by BA and RM increased the start and end times of setting of the mortars. Still, these times of setting were in accordance with the values mentioned in ASTM C1708 [10]. They were considered adequate for the workability conditions (90 to 180 min) and hardening (up to 240 min), defined in this study. The delay in mortar setting times was also verified when PC is replaced by BA fines [21]. On the other hand, LF particles can act as nucleation points, where hydration products can precipitate and, in this way, increase the rate of hydration reactions [39]. Therefore, the replacement of LF by BA and RM benefits the cases that demand more time for transport and application of the material. The delay in setting time may be related to the internal curing process, in which the evolution of hydration reactions occurs more slowly, as the water initially absorbed by the BA and RM fines are made available in the mixture. The SLUs with BA showed longer setting times in relation to the SLUs with RM, indicating that the gradual availability of water may have occurred with greater intensity or for a longer period due to the high porosity of the BA particles.

Table V - Flows and setting times of mortars with LF, BA, and RM additions.

SLU	SP (%)	VMA (%)	SR (%)	F (cm)	SS (min)	ES (min)
0.2_LF	0.30	0.07	0.05	11.8	90	130
0.2_BA	0.30	0.20	0.05	11.4	110	170
0.2_RM	0.35	0.08	0.05	11.6	105	145
0.3_LF	0.32	0.04	0.05	11.8	90	130
0.3_BA	0.34	0.25	0.05	11.2	115	170
0.3_RM	0.39	0.05	0.05	11.1	95	135

Water absorption by immersion: the results of water absorption and void rates of SLUs with LF, BA, and RM additions at 28 days of curing are shown in Fig. 4. The replacement of LF by BA and RM had no influence on the water absorption and void ratio values in both levels of additions. Among the mixtures evaluated, only SLUs with 0.2 addition of red mud (0.2_RM) showed significantly higher porosity than SLUs with 0.3 addition of LF and BA (0.3_LF and 0.3_BA). These results indicated that the content and type of addition incorporated into the CAC/FGD/PC system influenced the porosity of SLUs, because of packaging and/or hydration products.

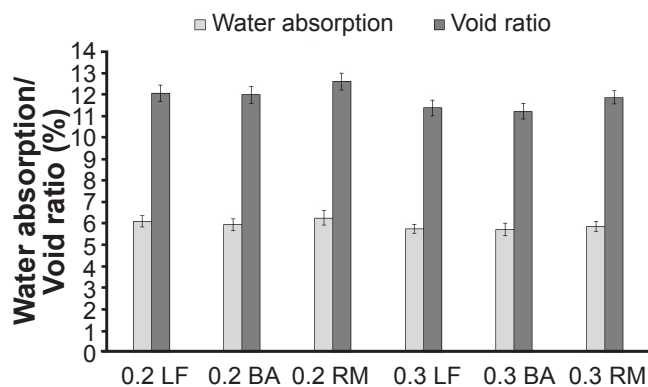


Figure 4: Water absorption and void ratio of SLUs with LF, BA, and RM additions.

Mechanical (flexural and compressive) strengths: the flexural tensile and compressive strength results of SLUs with the addition of LF, BA, and RM are shown in Figs. 5a and 5b, respectively. All mortars produced showed high mechanical (flexural and compressive) strength, in accordance with the values defined in ASTM C1708 [10], at all ages tested. It is noteworthy that the compressive strength values obtained at 1 day of curing were higher compared to the values reported at 1 day of curing of PC-based SLUs [41], and close compared to the values reported at 7 days of curing of PC-based SLUs [42]. At the initial curing age (1d), the replacement of LF by BA and RM promoted an increase in the compressive strength values, mainly for higher addition contents. Based on the lowest end times of setting observed in SLUs with LF addition, it was expected to obtain higher initial mechanical strengths in these systems. These results indicated that the BA and RM particles promoted a better initial curing process, attributed to the internal curing phenomenon. In the case of BA, the higher porosity of its particles may have promoted the reduction of the initial availability of water in the mixture due to its rapid absorption. In the case of red mud, the greater specific area of its particles, in relation to LF and BA, and its greater porosity, in relation to LF, may also have reduced the initial availability of water. Therefore, the reduction of the initial water content of the mixture, followed by the gradual release of the initially absorbed water, may have benefited the hydration process. Considering the standard deviations presented at 28 days of curing, the replacement of LF by BA and RM showed no significant influence on the values of the mechanical (flexural and compressive) strengths of SLUs, in both levels of tested additions. The treatments performed in this study benefited the pozzolanic activity of BA [17] and that of RM [26]. Therefore, replacing LF by BA and RM could increase the compressive strengths at advanced curing ages (28d). The reason why the replacement of LF by BA and RM did not significantly influence the values of compressive strength at 28 days of curing was attributed to the low availability of portlandite (CH), which is essential for pozzolanic reactions to occur. The low availability of the CH phase was related to the low PC content (20%) adopted in this study's CAC/FGD/PC system, which resulted in the

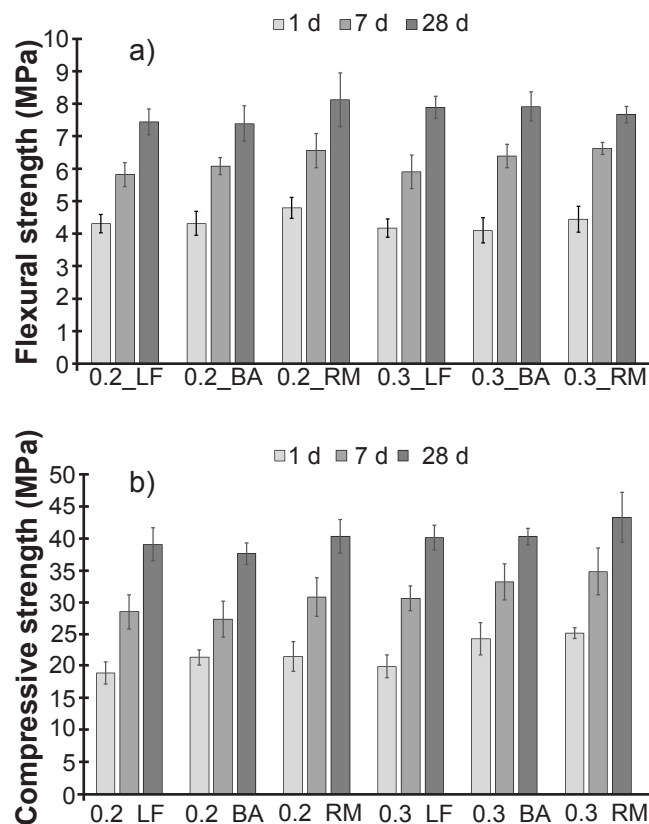


Figure 5: Flexural (a) and compressive (b) strengths of SLUs with LF, BA, and RM additions.

formation of low CH levels compared to a PC-based system. Additionally, the hydration reactions of the CAC/FGD/PC system (Eq. A) also consumed CH.

Mineralogical analyses: the X-ray diffractograms of the pastes based on the CAC/FGD/PC/LF, CAC/FGD/PC/BA, and CAC/FGD/PC/RM systems with 0.2 and 0.3 additions at 28 days of curing are respectively shown in Figs. 6a, 6b, and 6c. Based on the qualitative analysis of the diffractograms presented, it was found that the replacement of LF for BA and RM influenced the hydration products. Therefore, the evaluated fines presented reactivity with the adopted binder system (CAC/FGD/PC). For the reference paste (LF), the hydration products that presented crystalline phases were: ettringite, monosulfate, and hemihydrate. In turn, the crystalline phases formed in the pastes with replacement of LF by BA and RM were ettringite, stratlingite, and/or monosulfate. In CSA/C\$/PC system, stratlingite can be formed from the hydration reactions of the belite phase with amorphous aluminum hydroxide (Eq. H) [36]. Furthermore, the conversion of ettringite and CAH_{10} to stratlingite and monosulfate can occur under the consumption of C_3S (Eq. I) [36]. In CAC/FGD/PC system, the formation of stratlingite can also occur from the hydration of the gehlenite phase (C_2AS), coming from CAC (Eq. J). In this system (CAC/FGD/PC), stratlingite crystallization was not detected after 24 h of hydration since gehlenite has low hydraulic activity [43]. In CAC/C\$/PC system, the formation of the stratlingite

phase was detected after 3 days of curing and occurred in temperature conditions above 20 °C. In this case (CAC/C\$/\$PC), the intensity of the stratlingite and gibbsite (AH₃) phases were higher in pastes cured at 40 °C [44].



In the present study, for 0.2 LF replacement, stratlingite was detected in the pastes with BA and RM residues,

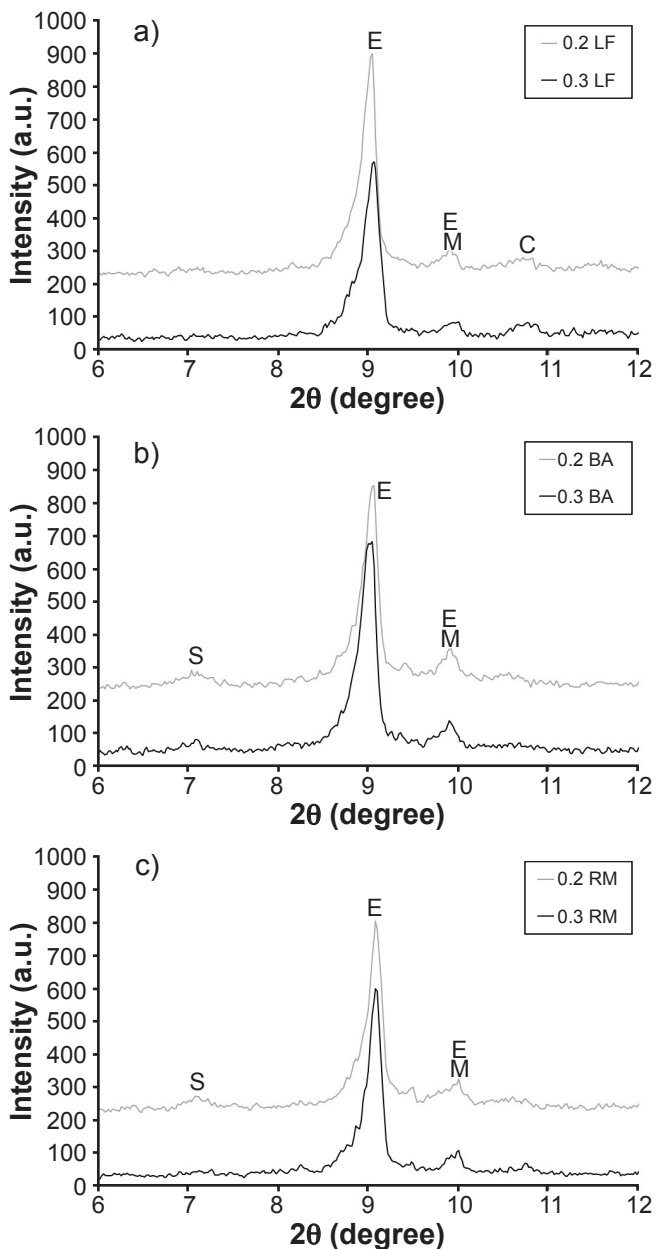


Figure 6: X-ray diffractograms of the pastes based on the CAC/FGD/PC/LF (a), CAC/FGD/PC/BA (b), and CAC/FGD/PC/RM (c) systems. E: ettringite ($C_6A\bar{S}_3H_{32}$), M: monosulfate ($C_4A\bar{S}H_{18}$), C: hemicarboaluminate ($C_4AC_0.5H_{11}$), S: stratlingite (C_2ASH_8).

indicating that the presence of silicon influenced the formation of this phase. However, stratlingite was not detected in the paste with 0.3 replacement of LF for RM, and the paste with the highest content of bottom ash (0.3_BA) showed a lower content of the stratlingite phase (Fig. 7), in relation to the pastes with lower bottom ash contents (0.2_BA). This result may be related to the lower contents of binders and the lower w/f ratio of the pastes with 0.3 addition since higher w/c ratios favor the formation of a higher content of stratlingite, in pastes based on of the BYF system (belite, ye'elemite, and ferrite) [45]. Likewise, the absence of the stratlingite phase in the paste with the highest RM content (0.3_RM) reinforced the evidence that the availability of silicon influenced the formation of stratlingite since this phase was detected in the paste with the highest BA content (0.3_BA), which had approximately twice the silicon oxide content (SiO₂) in relation to RM (Table II). The results of semi-quantitative analysis associated with the peak areas of the phases are shown in Fig. 7. E_M is the peak area associated with the overlap of the ettringite and monosulfate phases ($2\theta \approx 10^\circ$). In general, the pastes showed similar contents of the main phase (E), ranging from 84% to 91%. For 0.2 addition, the replacement of LF by BA and RM resulted in a reduction in the area associated with the main ettringite peak, indicating that a lower content of this phase was formed. Given this result, the increase in the peak area associated with the overlap of the ettringite and monosulfate (E_M) phases, due to the replacement of 0.2 of LF for BA and RM, suggested that the pastes with the residues (BA and RM) formed higher levels of monosulfate, in relation to the reference (0.2_LF). In turn, the replacement of 0.3 of LF by BA and RM did not show any influence on the content of ettringite formed. However, it suggested an increase in the monosulfate content. Thus, as observed in the pastes with 0.2 addition, the lower contents associated with the monosulfate and the presence of the hemicarboaluminate (C) showed that the CAC/FGD/PC system with LF addition had a better ability to stabilize ettringite compared to the evaluated residues (BA and RM).

Drying shrinkage: the drying shrinkage and mass loss values of SLUs with LF, BA, and RM additions are

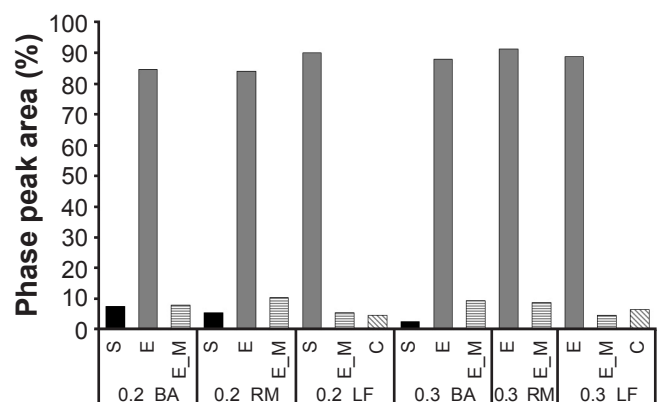


Figure 7: Phases' peak areas according to the XRD patterns.

respectively shown in Figs. 8a and 8b. At all curing ages, the mortars produced showed drying shrinkage values lower than the values defined in ASTM C1708 [10], proving that the binder system adopted showed good performance in compensating for drying shrinkage. At 28 days of curing, the highest drying shrinkage values shown in Fig. 8a (0.3_RM) were close to the lowest values obtained in SLUs based on CAC/C\$/PC system with high PC contents [2], and 10 times smaller compared to those obtained with self-leveling PC-based underlayments [41]. Mortars with 0.2 replacement of LF by BA and RM showed lower mass loss at the initial curing age (3d, Fig. 8b), indicating that the fines of the tested residues may have reduced the loss of water to the environment (internal curing), thus contributing to the reduction of shrinkage by initial drying (3d). However, mortars with 0.3 replacement of LF by BA and RM did not reduce water loss at the initial curing age (3d). This result may be associated with the greater gradual release of water in systems with higher levels of residues (0.3_BA and 0.3_RM).

The replacement of 0.2 LF by BA and RM residues reduced the drying shrinkage values of the SLUs, and dimensional stability was achieved at 14 days of curing. Considering that the void ratios of SLUs with 0.2 addition did not show a significant difference, the dimensional variation over time was related to the packing effects of the additions and with the hydration products since they influence the pore size distribution. The dimensional variations between 3 and 14 days of curing were lower in the reference mortar (0.2_LF). These results were consistent with the highest levels of ettringite and the lowest levels of monosulfate, indicated in the XRD analyses on the paste of this system (0.2_LF). After 14 days of curing, the mortars with the residues (0.2_BA and 0.2_RM) showed less dimensional variation, especially those with bottom ash. The replacement of 25% of BYF (belite, ye'elemite, and ferrite) cement by fly ash has been shown to promote a pore refinement effect due to the formation of stratlingite and ettringite at more advanced ages [45]. Considering that the paste with bottom ash (0.2_BA) showed the highest content of stratlingite, this phase may have benefited the dimensional stability after 14 days of curing since its crystallization can promote the refinement of the pores. The replacement of 0.3 LF by BA and RM promoted an increase in drying shrinkage values. Since systems with 0.3 addition showed similar ettringite contents, as well as similar initial mass loss (3d) values, the highest dimensional variations observed in mortars with higher residue contents (0.3_BA and 0.3_RM) may be related to the increase in the conversion reactions of ettringite into monosulfate (Eqs. E and F). In other words, the best ettringite stabilization process suggested in the XRD analyses of the reference paste (0.3_LF) seems to have been a good parameter to control the dimensional variation of the SLUs with 0.3 addition. Besides, the packing effects of the additions may also be involved, as they influence the pore size distribution, which may be one of the reasons why SLUs with higher bottom ash contents (0.3_BA) showed

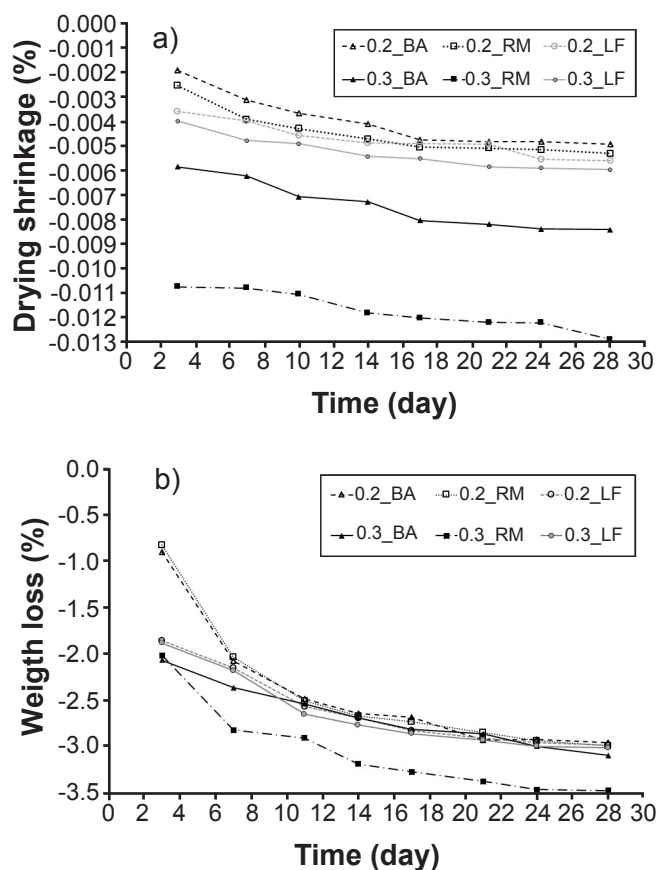


Figure 8: Drying shrinkage (a) and mass loss (b) of SLUs with LF, BA, and RM additions.

lower drying shrinkage values compared to SLUs with higher red mud contents (0.3_RM).

CONCLUSIONS

The initial mechanical (flexural and compressive) strengths (1d) of self-levelling underlayments (SLUs) based on CAC/FGD/PC (calcium aluminate cement/calcium sulfate derived from the flue gas desulfurization process/Portland cement) system were higher in compositions with 20% PC when compared to compositions with 10% PC. For 20% PC, SLUs with CAC/FGD ratios of 2.33 and 3.00 promoted higher flexural strength values at 7 days of curing and lower linear shrinkage at 28 days compared to SLUs with CAC/FGD ratio of 4.00. The influences of replacing limestone filler (LF) by bottom ash (BA) and red mud (RM) residues on the properties of SLUs, based on the CAC/FGD/PC system (56/24/20), were: i) the replacement of LF by BA and RM benefited the initial compressive strength (1d), mainly in SLUs with higher replacement contents (0.3_BA and 0.3_RM) since the characteristics of bottom ash particles (porosity) and red mud (surface area) promoted the reduction of the initial w/f [water/(CAC+FGD+PC+LF)] ratio, followed by the gradual availability of water to the system (internal curing); ii) the replacement of LF by BA and RM influenced the hydration products; the crystallization of

stratlingite was influenced by the type and content of the residue (BA and RM) and did not occur in the paste with LF; iii) the replacement of 0.2 LF by BA and RM reduced the initial values of mass loss and drying shrinkage (3d) of the SLUs, indicating that when the residue content is adequate, the internal curing effect can benefit the initial dimensional stability of the CAC/FGD/PC system; and iv) all mortars produced with additions of bottom ash (CAC/FGD/PC/BA) and red mud (CAC/FGD/PC/RM) showed adequate fluidity, setting times, mechanical (flexural and compressive) strength, and linear drying shrinkage, and may even enhance the SLUs properties, in relation to PC-based and CAC/FGD/PC/LF-based SLUs, provided that the residue contents (FGD, BA, and RM) are properly dosed.

ACKNOWLEDGEMENTS

The authors would like to thank the National Council for Scientific and Technological Development (CNPq) and CAPES for the financial support to this study. The authors are also grateful for the XRD measurements of the binders and additions conducted at the multi-user LDRX facility at UFSC, the XRD measurements of the pastes conducted in the UFSC Nanotechnology laboratory, and the BET measurements conducted at the chemical and food engineering EQA analysis center at UFSC.

REFERENCES

- [1] L. Yang, Y. Zhang, Y. Yan, *J. Clean. Prod.* **127** (2016) 204.
- [2] S. Zhang, X. Xu, S.A. Memon, Z. Dong, D. Li, H. Cui, *Constr. Build. Mater.* **167** (2018) 253.
- [3] K. Onishi, T.A. Bier, *Cem. Concr. Res.* **40** (2010) 1034.
- [4] T. Emoto, T.A. Bier, *Cem. Concr. Res.* **37** (2007) 647.
- [5] S. Seifert, J. Neubauer, F. Goetz-Neunhoeffler, *Cem. Concr. Res.* **42** (2012) 919.
- [6] J. Péra, J. Ambroise, *Cem. Concr. Res.* **34** (2004) 671.
- [7] J.F. Georgin, J. Ambroise, J. Péra, J.M. Reynouard, *Cem. Concr. Compos.* **30** (2008) 769.
- [8] O. Coussy, *Mechanics and physics of porous solids*, John Wiley, France (2010).
- [9] J. Yang, L. Liu, Q. Liao, J. Wu, J. Li, L. Zhang, *Constr. Build. Mater.* **201** (2019) 401.
- [10] C1708, “Standard test methods for self-leveling mortars containing hydraulic cements”, ASTM (2019).
- [11] M. Deng, M. Tang, *Cem. Concr. Res.* **24** (1994) 119.
- [12] L. Xu, N. Li, R. Wang, P. Wang, *Constr. Build. Mater.* **163** (2018) 225.
- [13] C.O. Schaefer, M. Cheriaf, J.C. Rocha, *Materials* **10** (2017) 958.
- [14] D.Y. Lei, L.P. Guo, W. Sun, J.P. Liu, C.W. Miao, *Constr. Build. Mater.* **153** (2017) 765.
- [15] P. Córdoba, *Fuel* **144** (2015) 274.
- [16] L. Moonen, B.V. Novem, *Waste Mater. Constr.* **48** (1991) 507.
- [17] M. Cheraif, J.C. Rocha, J.C. Péra, *Cem. Concr. Res.* **29** (1999) 1387.
- [18] M. Rafeizonooz, J. Mirza, M.R. Salim, M.W. Hussin, E. Khankhaje, *Constr. Build. Mater.* **116** (2016) 15.
- [19] H.K. Kim, *Constr. Build. Mater.* **91** (2015) 57.
- [20] H.K. Kim, H.K. Lee, *Constr. Build. Mater.* **25** (2011) 1115.
- [21] S. Oruji, N.A. Brake, L. Nalurri, R.K. Guduru, *Constr. Build. Mater.* **153** (2017) 317.
- [22] L. Wu, N. Farzadnia, C. Shi, Z. Zhang, H. Wang, *Constr. Build. Mater.* **149** (2017) 62.
- [23] R.X. Liu, C.S. Poon, *J. Clean. Prod.* **112** (2016) 384.
- [24] R.X. Liu, C.S. Poon, *J. Clean. Prod.* **135** (2016) 1170.
- [25] J. Yang, B. Xiao, *Constr. Build. Mater.* **22** (2008) 2299.
- [26] E.P. Manfroi, M. Cheriaf, J.C. Rocha, *Constr. Build. Mater.* **67** (2014) 29.
- [27] NBR 16607, “Cimento Portland: determinação dos tempos de pega”, ABNT, Rio Janeiro (2018).
- [28] NBR 7215, “Cimento Portland: determinação da resistência à compressão de corpos de prova cilíndricos”, ABNT, Rio Janeiro (2019).
- [29] NBR 13279, “Argamassa para assentamento e revestimento de paredes e tetos: determinação da resistência à tração na flexão e à compressão”, ABNT, Rio Janeiro (2005).
- [30] NBR 9778, “Argamassa e concreto endurecidos: determinação da absorção de água, índice de vazios e massa específica”, ABNT, Rio Janeiro (2009).
- [31] P.E. Manfroi, “Desenvolvimento de aglomerantes ecoeficientes com encapsulamento de metais pesados”, Dr. Thesis, UFSC, Florianópolis (2014).
- [32] C.A.A. Rocha, “Influência da pressão e temperatura de cura e da adição de NaCl e KCl no comportamento de pastas para cimentação de poços de petróleo”, Dr. Thesis, UFRJ, Rio Janeiro (2015).
- [33] J. Zhang, G.W. Scherer, *Cem. Concr. Res.* **41** (2011) 1024.
- [34] K.L. Scrivener, A. Campas, in “Lea’s chemistry of cement and concrete”, P.C. Hewlett (Ed.), 4th ed., Oxford (1998) 713.
- [35] I. Older, in “Lea’s chemistry of cement and concrete”, P.C. Hewlett (Ed.), 4th ed., Oxford (1998) 241.
- [36] J.J. Wolf, D. Jansen, F. Goetz-Neunhoeffler, J. Neubauer, *Cem. Concr. Res.* **147** (2021) 106496.
- [37] T.D. Martin, “Mezclas ternarias de cemento Portland, cemento de aluminato de calcio y sulfato cálcico: mecanismos de expansión”, Dr. Thesis, UPC, Barcelona (2013).
- [38] J.S. Andrade Neto, A.G. Torre, A.P. Kirchheim, *Constr. Build. Mater.* **279** (2021) 122428.
- [39] D. Wang, C. Shi, N. Farzadnia, Z. Shi, H. Jia, Z. Ou, *Constr. Build. Mater.* **181** (2018) 659.
- [40] J. Bizzozero, K.L. Scrivener, *Cem. Concr. Res.* **76** (2015) 159.
- [41] T.P. Scolaro, J.C. Rocha, *Cerâmica* **67**, 382 (2021) 179.
- [42] M.A.S. Anjos, T.R. Araújo, R.L.S. Ferreira, C.E. Farias, A.E. Martinelli, *J. Build. Eng.* **32** (2020) 101694.
- [43] W. Lou, B. Guan, Z. Wu, *J. Therm. Anal. Calorim.* **101** (2010) 119.

[44] L. Xu, K. Wu, C. Robler, P. Wang, H.M. Ludwig, *Cem. Concr. Compos.* **80** (2017) 298.

(*Rec.* 05/08/2021, *Rev.* 26/10/2021, 23/12/2021, *Ac.* 29/12/2021)

[45] G.Y. Koga, B. Albert, P.N. Nogueira, *Cem. Concr. Res.* **137** (2020) 106215.

